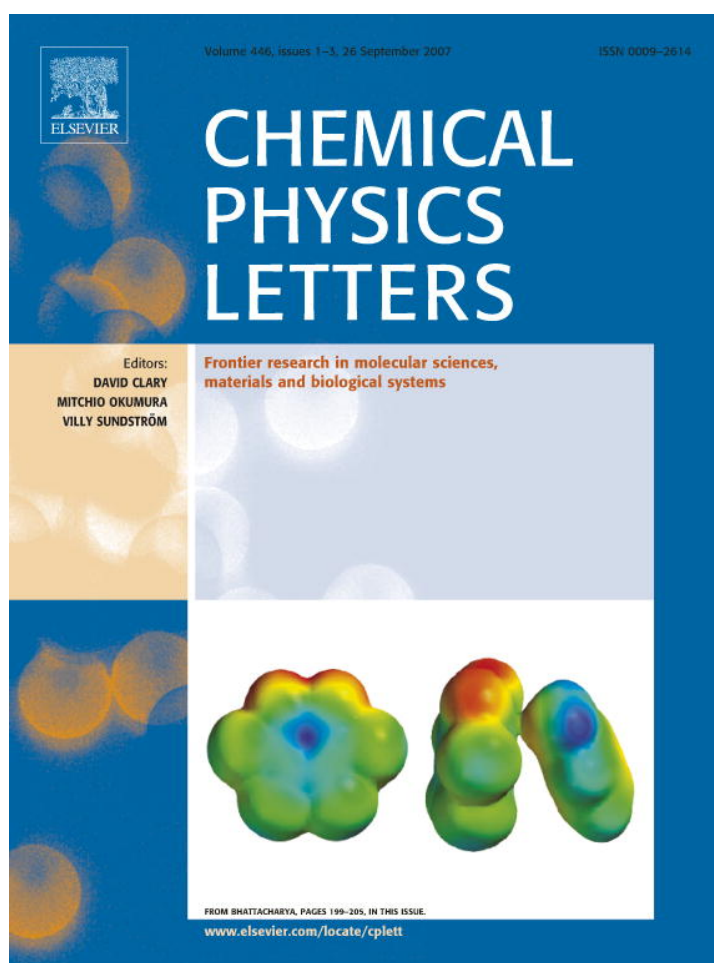


Provided for non-commercial research and education use.  
Not for reproduction, distribution or commercial use.



This article was published in an Elsevier journal. The attached copy is furnished to the author for non-commercial research and education use, including for instruction at the author's institution, sharing with colleagues and providing to institution administration.

Other uses, including reproduction and distribution, or selling or licensing copies, or posting to personal, institutional or third party websites are prohibited.

In most cases authors are permitted to post their version of the article (e.g. in Word or Tex form) to their personal website or institutional repository. Authors requiring further information regarding Elsevier's archiving and manuscript policies are encouraged to visit:

<http://www.elsevier.com/copyright>



# The effects of extensive pitting on the mechanical properties of carbon nanotubes

Steven L. Mielke<sup>a,\*</sup>, Sulin Zhang<sup>b,1</sup>, Roopam Khare<sup>b</sup>, Rodney S. Ruoff<sup>b</sup>,  
Ted Belytschko<sup>b</sup>, George C. Schatz<sup>a</sup>

<sup>a</sup> Department of Chemistry, Northwestern University, Evanston, IL 60208-3113, USA

<sup>b</sup> Department of Mechanical Engineering, Northwestern University, Evanston, IL 60208-3111, USA

Received 12 June 2007; in final form 8 August 2007

Available online 15 August 2007

## Abstract

As previously demonstrated, a single hole is sufficient to markedly reduce the fracture strength of a carbon nanotube (CNT). Herein we present calculations exploring the effects of multiple holes on the modulus, fracture strength, and fracture strain of CNTs. The modulus decreases sharply and approximately linearly as a function of the pitting density. A few holes cause a decrease in the failure strain but extensive pitting leads to higher failure strains. These results suggest that the unusually low modulus measurements and high failure strains reported in the experiments of Yu et al. [Science 287 (2000) 637] were a consequence of purification induced oxidative pitting. © 2007 Elsevier B.V. All rights reserved.

## 1. Introduction

Quantum mechanical (QM) calculations [1–6] predict that defect-free carbon nanotubes (CNTs) have Young's modulus values of  $\sim 1$  TPa, fracture strengths of  $\sim 100$  GPa, and failure strains of  $\sim 20$ – $30\%$  depending on their chirality, with generally good agreement existing between the predictions of tight binding [1,2,5], semiempirical [3,4,6], and density functional theory [5,6] methods. A number of experimental studies [7–12] have been conducted for CNT fracture, but agreement both between the experimental results and between theory and experiment is limited. Some of the experiments [8–10] involved multiwalled CNTs (MWCNTs) for which more than one shell is load bearing, and this complicates experimental–theoretical comparisons. Two experiments [7,11] reported fracture

studies of arc-discharge-grown MWCNTs, and only the outermost shell was load bearing for those samples. The experiment of Yu et al. [7] reported 19 fracture strength measurements ranging from 11 to 63 GPa (with a mean value of 28 GPa), four modulus measurements of 950, 470, 335, and 274 GPa, and four failure strain measurements, one below 3% and three between 11% and 13%. The later experiment of Ding et al. [11] reported data for 14 MWCNTs with fracture strengths ranging from 10 to 66 GPa (with a mean value of 24 GPa), modulus measurements ranging from 620 to 1200 GPa (with a mean value of 955 GPa), and failure strains ranging from 1.0% to 6.3% (with a mean value of 2.6%).

The discrepancy between theory and experiment for the fracture strengths has received the most attention, and early theories [13] focused on stress-induced Stone–Wales defects [14] as the likely cause of the low strength measurements. It was eventually realized that even though Stone–Wales defects become energetically favorable at higher strains, the transformation barriers remain sufficiently high [4,15] that such processes could not explain fracture measurements at room temperature. It was subsequently observed [6,16,17] that the MWCNTs used in the

\* Corresponding author. Fax: +847 491 7713.

E-mail addresses: [slmielke@chem.northwestern.edu](mailto:slmielke@chem.northwestern.edu) (S.L. Mielke), [r-ruoff@northwestern.edu](mailto:r-ruoff@northwestern.edu) (R.S. Ruoff), [tedbelytschko@northwestern.edu](mailto:tedbelytschko@northwestern.edu) (T. Belytschko), [schatz@chem.northwestern.edu](mailto:schatz@chem.northwestern.edu) (G.C. Schatz).

<sup>1</sup> Present address: Department of Mechanical Engineering, 204 Mechanical Engineering Building, University of Arkansas, Fayetteville, AR 72701, USA.

Yu et al. [7] experiments had been purified using an oxidative etching process [18] that was likely to introduce significant pitting that could easily explain the observed strength measurements.

The anomalously low modulus measurements and high failure strains reported by Yu et al. [7] have received less attention, although there has been speculation [19] that slippage at the cantilever-CNT attachment could explain these results (although there was never experimental evidence showing such slippage, it also was non-trivial to prove that slippage never occurred). In the subsequent experiments of Ding et al. [11], which used the same electron beam induced deposition (EBID) clamp-attachment procedure as used earlier, the clamp-attachment sites were carefully monitored for the possibility of slippage and this complication was demonstrated to be negligible. The primary distinction between the experimental procedures of Ding et al. [11], where the modulus measurements were more reasonable, and that of the earlier work of Yu et al. [7], was the use of unpurified CNTs. This suggests that extensive oxidative pitting is a more plausible hypothesis for the cause of the anomalous modulus and failure strain measurements in the work of Yu et al. [7] than slippage at the clamps. In the following, we present molecular mechanical (MM) calculations to indicate that a significant density of holes would indeed lead to both dramatically lower modulus and higher failure strain measurements.

## 2. Calculations, results, and discussion

A number of experiments [20–23] have demonstrated that exposing vacancy-defected graphite to oxygen at elevated temperatures leads to the formation of roughly circular holes in the surface graphene sheet. Oxidative etching is employed in many purification procedures [24,25] for CNTs as a way of removing amorphous carbon, soot, and seriously defected nanoparticles, but its use may lead to pitting in even high-quality CNTs due to the presence of a few vacancy defects. The distribution and types of defects that occur in CNTs and the specific mechanisms whereby these are oxidatively etched into holes are not fully-understood issues and, in any event, the details are likely to depend strongly on the specifics of the synthetic method employed; thus, a detailed model of realistic pitting patterns would be a difficult task. It has already been demonstrated [6,16,26] that a single significant hole is sufficient to dramatically reduce the fracture strength of a CNT to within the experimentally observed ranges. However, in order to affect the modulus, a significant density of defects would be required. In the calculations presented here, we will consider a very simple model of pitting in an attempt to understand some of the qualitative effects of multiple holes on the mechanical properties of CNTs.

Multiscale QM/MM calculations for the fracture of a large CNT are affordable when the vicinity of a single hole is treated via QM methods [26] but it would be prohibitively expensive to study CNTs containing many holes in

this manner. Instead, we choose to model our CNTs purely at the MM level using a modified second-generation reactive empirical bond order (REBO) potential [27] of Brenner and coworkers. The modified potential will be denoted MTB-G2, and it is obtained [19,28] by removing the cutoff functions of the standard REBO potential and instead considering only interatomic interactions between atom pairs that lie within 2.0 Å of each other in the initial unstrained structure. This modification renders the potential incapable of treating bond formation but prevents highly anomalous fracture behavior. The MTB-G2 potential can yield qualitatively incorrect results for certain types of defected structures [3], and generally tends to underestimate the modulus, fracture strength, and failure strains of CNTs. However, for vacancy defects and holes the potential has been shown to do an acceptable job of estimating the fractional strength reductions, i.e.,  $\sigma_{\text{defected}}/\sigma_{\text{pristine}}$ , when compared to QM and QM/MM benchmarks [6,26].

We restrict attention to [15,15] armchair CNTs pitted via random distributions of the smallest possible circular holes, namely the removal of all six carbon atoms from the same hexagonal ring. We emphasize that the choice of these defects is motivated entirely by convenience; chemically-motivated defect choices would lead to much more complicated structures requiring explicit treatment of oxygen-containing functional groups. We use periodic boundary conditions and consider a unit cell consisting of 3000 carbon atoms prior to pitting. Hexagonal rings are removed randomly and sequentially (adjacent holes are permitted; thus, the largest defect can be larger than one-hexagon in size) until a desired defect density is achieved; additionally, any carbon atom retaining less than two of its initial nearest neighbors is removed, and at the final stage all dangling bonds are saturated with hydrogen atoms. We define the pitting density,  $f$ , for a particular tube as the fraction of the initial 3000 carbon atoms that are removed by this process. The initial pitted structures are optimized to determine the zero-strain configuration, and then axial tension is applied in strain increments of 0.1%, followed by geometry optimization, until segmentation occurs. Young's modulus values and engineering stresses are computed directly from the energies via finite differences. An effective shell thickness of 3.4 Å is used in defining the moduli and stresses, and the initial radius that is used in the definition of the engineering stresses is taken as that of the optimized value of a defect-free tube (10.18 Å). The failure stress is defined as the maximum observed stress and the failure strain is defined as the engineering strain for which the maximum stress is observed; in many cases further extension of the tube beyond the failure strain does not lead to immediate segmentation.

A plot of the effective modulus,  $Y'$ , as a function of the pitting density,  $f$ , is given in Fig. 1a, a plot of the failure stress as a function of  $f$  is given in Fig. 1b, and a plot of the failure strain as a function of  $f$  is given in Fig. 1c. For the unit cell size chosen here a single hole corresponds to  $f = 0.002$ . For reference, the modulus, failure stress, and

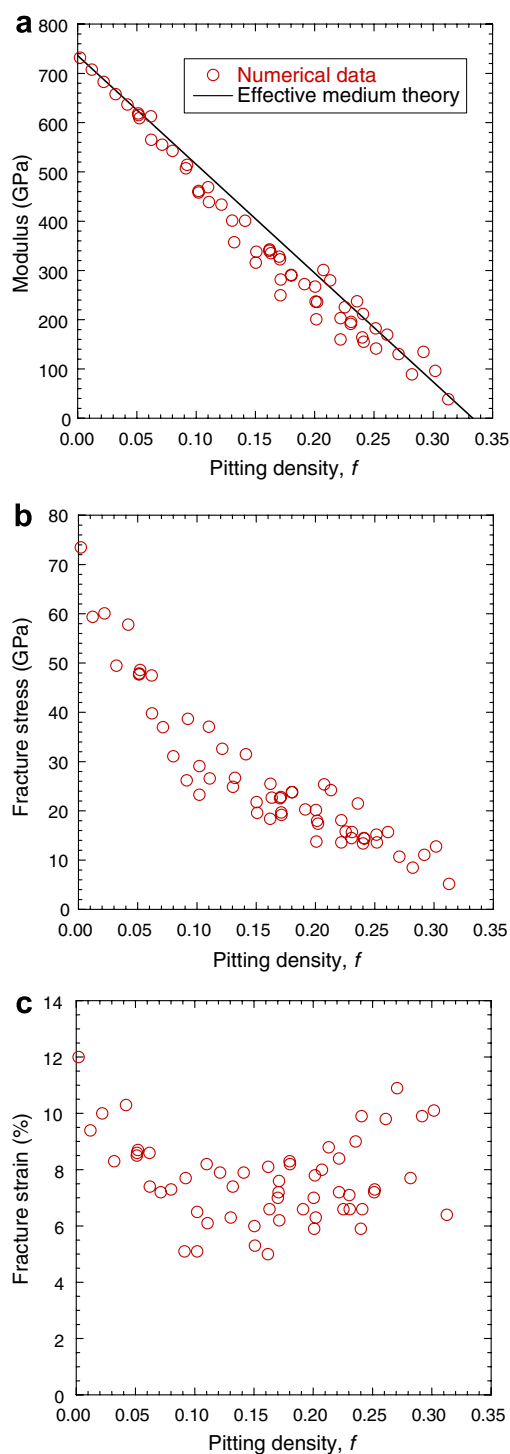


Fig. 1. The open circles are numerical data indicating the trends in the mechanical properties as a function of the pitting density: (a) Young's modulus, (b) fracture stress, (c) failure strain. The line in (a) is the effective medium prediction of Eq. (1) when the hole volume fraction is estimated by the pitting density.

failure strain of a pristine [15] CNT as predicted by the MTB-G2 potential are 736 GPa, 105.7 GPa, and 29.8%, respectively.

As seen in Fig. 1a, the effective modulus,  $Y'$ , declines nearly linearly as a function of the pitting density. A num-

ber of continuum effective medium theories (EMT) [29] have been proposed that can be applied to composite continua containing inclusions and similar approximations have been obtained based on fracture mechanics ideas [30]. In particular, Thorpe and Sen [31] showed that for the special case of circular voids in a two-dimensional sheet the Young's modulus within the self-consistent approximation (SCA) [32,33] is given by

$$Y'(\phi) = Y(1 - 3\phi), \quad (1)$$

where  $Y'$  is the effective modulus of the pitted system,  $Y$  is the modulus of the defect-free material, and  $\phi$  is the volume fraction of holes. The EMT formulas are valid in the limit of low defect densities, and they clearly break down at high densities as can be seen by the inaccuracy of the percolation limit values: Eq. (1) predicts a percolation limit of  $\phi = 1/3$ , whereas numerical calculations for randomly distributed voids indicate a percolation limit of about 0.68 [34] and calculations for voids with centers chosen from a lattice indicate a percolation limit of about 0.60 [35]. Herein we only consider pitting densities below about 30%, which is sufficient to span the regime appropriate for comparison to the available experiments; the percolation limit for the atomistic pitting scheme presumably occurs at significantly higher pitting densities.

If we estimate the volume fraction of holes for an atomistic material by  $f$ , the initial reduction of the fractional modulus,  $Y'(f)/Y$ , of our numerical calculations, of about  $3.25f$  (estimated from a linear fit of the first five points), shows excellent agreement with the EMT prediction of  $3f$  indicated in Eq. (1). The modulus reduction is roughly linear in  $f$  up to at least  $f = 20\%$ , and the numerical results are systematically smaller than the EMT predictions. At higher pitting densities the rate of decline of the modulus begins to slow, but by  $f = 30\%$  the effective modulus is only 10–20% of its initial value.

As shown in Fig. 1b, the fracture stress declines sharply with increasing  $f$  for low pitting densities but the rate of decline slows after about  $f = 10\%$ . These strength decreases are due to two effects: the overall decrease in the modulus and the patterns of larger defects that result at higher pitting densities. A single isolated hole within our unit cell leads to a fracture stress of 73.5 GPa, which is about a 30% decrease from the strength of the defect-free CNT. A few isolated holes, in a CNT with a pitting density of  $f$ , lead to fracture strengths that are very close to a factor of  $Y'(f)/Y$  times the strength of a CNT with a single isolated one-hexagon hole. As the pitting density increases the likelihood of adjacent holes leading to larger defects increases, and these larger defects can lead to significantly greater weakening than isolated defects – at low defect densities the worst defect is typically the strength-limiting feature of a CNT.

It is important to realize that size alone does not determine what constitutes the worst defect. Removing two hexagons that are adjacent in the circumferential direction (from an otherwise defect-free tube) leads to a fracture

strength of  $\sim 57$  GPa at  $\sim 8.7\%$  strain, which is a 22% reduction from the strength of a CNT with a single-hexagon hole, whereas removing two hexagons that are adjacent in the axial direction leads to a fracture strength of  $\sim 75$  GPa, which is slightly stronger than the strength of a CNT with a single-hexagon hole. Of the 58 defect patterns considered here, the fracture strength is never lower than 0.51 times the strength we would expect for a CNT with isolated hexagonal holes and the observed modulus, i.e.,  $Y'(f)/Y$  times the strength of a CNT with a single-hexagon hole. Thus, the decline in the modulus as the pitting density increases typically plays a more important role in determining the fracture strength than the clustering of defects does.

As seen in Fig. 1c, the failure strains initially decline with  $f$  and display a wide variation for a given pitting density, but tend toward a minimum in the range of roughly  $f = 10\text{--}15\%$  and thereafter tend to increase with increasing  $f$ . The lowest failure strain observed in the 58 defect patterns considered here was 5.0%. For a CNT with a single hole, we would expect the failure strain to monotonically decrease as the diameter of the hole increases and for irregularly-shaped defects we would still expect a strong correlation between larger defects and lower failure strains. At low defect densities the failure tends to be straightforwardly determined by the worst defect; thus, the initial decline in the failure strain with increasing  $f$  is the expected result. At high defect densities the tube possesses multiple large defects, each of which undergo large deformation, and this distributed-deformation behavior tends to lead to higher strains for a given stress value. Furthermore, at high values of  $f$ , localized bond failures in highly deformed regions can lead to the aggregation of nearby holes into larger defects without leading to fracture. Often, such defect aggregations provide a mechanism for significant stress reduction; thus, the stress–strain behavior of extensively-pitted CNTs is non-monotonic and failure is delayed to higher strain values. An example of this defect-aggregation behavior is shown in Fig. 2.

### 3. Concluding remarks

We have presented calculations showing the effects of pitting on the mechanical properties of CNTs. The modulus decreases sharply and approximately linearly as a function of the pitting density,  $f$ , and shows good agreement with the effective medium theory predictions for results below about  $f = 25\%$ . The fracture strength initially decreases with increasing  $f$  more rapidly than the modulus does because the size of the largest defect tends to increase with increasing  $f$ . At higher defect densities the presence of multiple large defects and failure modes involving aggregation of holes into larger defects lead to a decrease in the failure stress reduction rate with increasing  $f$  and an increase in the observed failure strains.

The presence of extensive pitting provides a plausible explanation for the low failure strengths as well as the low modulus values and high failure strains reported in

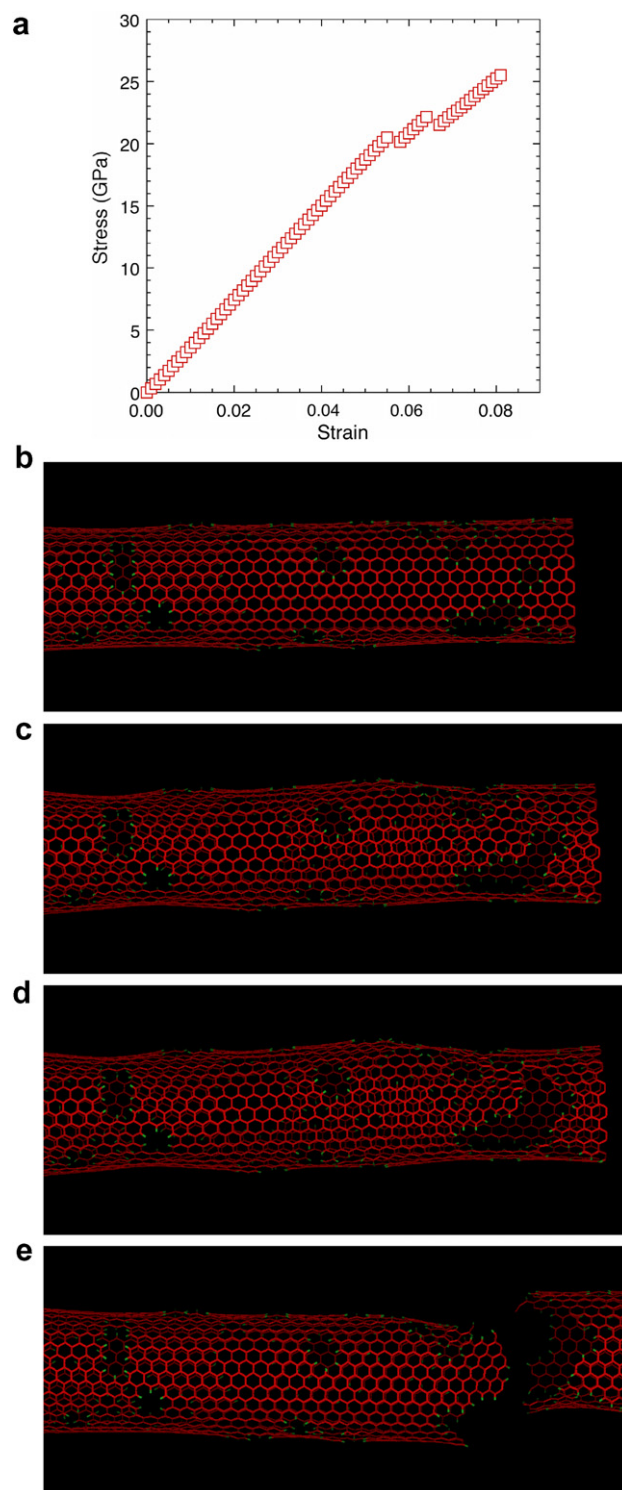


Fig. 2. The fracture mechanism for a tube with a pitting density of  $f = 0.16$  is displayed. The stress vs. strain curve is given in (a), a structure (carbon atoms are red and hydrogen atoms are green) at a strain of 0.056 is shown in (b), (c) shows a structure at a strain of 0.057, which is just after the aggregation of two holes near the right edge of the unit cell that leads to a modest stress reduction, (d) shows the structure at a strain of 0.066, where the large hole widens further leading to a second instance of stress reduction, and (e) shows the fully segmented tube. (For interpretation of the references in colour to this figure legend, the reader is referred to the web version of this article.)

the CNT fracture measurements of Yu et al. [7]. In fact, plausible pitting densities of 0.1–0.2 lead to the range of failure stresses of  $\sim 10$ – $30$  GPa, which corresponds to the failure stresses most commonly observed in the experiments. Alternative theories involving stress-induced Stone–Wales defects [13] cannot explain the modulus measurements and are not consistent with the much lower failure strains reported in the Ding et al. [11] measurements of unpurified CNTs.

### Acknowledgement

We gratefully acknowledge the grant support from the NASA University Research, Engineering, and Technology Institute on Bio Inspired Materials (BIMat) under Award No. NCC-1-02037.

### References

- [1] E. Hernández, C. Goze, P. Bernier, A. Rubio, *Phys. Rev. Lett.* 80 (1998) 4502.
- [2] T. Ozaki, Y. Iwasa, T. Mitani, *Phys. Rev. Lett.* 84 (2000) 1712.
- [3] D. Troya, S.L. Mielke, G.C. Schatz, *Chem. Phys. Lett.* 382 (2003) 133.
- [4] T. Dumitrica, T. Belytschko, B.I. Yakobson, *J. Chem. Phys.* 118 (2003) 9485.
- [5] S. Ogata, Y. Shibutani, *Phys. Rev. B* 68 (2003) 165409.
- [6] S.L. Mielke et al., *Chem. Phys. Lett.* 390 (2004) 413.
- [7] M.-F. Yu, O. Lourie, M.J. Dyer, K. Moloni, T.F. Kelly, R.S. Ruoff, *Science* 287 (2000) 637.
- [8] B.G. Demczyk, Y.M. Wang, J. Cumings, M. Hetman, W. Han, A. Zettl, R.O. Ritchie, *Mater. Sci. Eng. A* 334 (2002) 173.
- [9] A.H. Barber, I. Kaplan-Ashiri, S.R. Cohen, R. Tenne, H.D. Wagner, *Compos. Sci. Technol.* 65 (2005) 2380.
- [10] A.H. Barber, R. Andrews, L.S. Schadler, H.D. Wagner, *Appl. Phys. Lett.* 87 (2005) 203106.
- [11] W. Ding, L. Calabri, K.M. Kohlhaas, X. Chen, D.A. Dikin, R.S. Ruoff, *Exp. Mech.* 47 (2007) 25.
- [12] J.Y. Huang et al., *Nature* 439 (2006) 281.
- [13] B.I. Yakobson, *Appl. Phys. Lett.* 72 (1998) 918.
- [14] A.J. Stone, D.J. Wales, *Chem. Phys. Lett.* 128 (1986) 501.
- [15] Q. Zhao, M.B. Nardelli, J. Bernholc, *Phys. Rev. B* 65 (2002) 144105.
- [16] S. Zhang, S.L. Mielke, R. Khare, D. Troya, R.S. Ruoff, G.C. Schatz, T. Belytschko, *Phys. Rev. B* 71 (2005) 115403.
- [17] S.L. Mielke, T. Belytschko, G.C. Schatz, *Annu. Rev. Phys. Chem.* 58 (2007) 185.
- [18] D.T. Colbert et al., *Science* 266 (1994) 1218.
- [19] T. Belytschko, S.P. Xiao, G.C. Schatz, R.S. Ruoff, *Phys. Rev. B* 65 (2002) 235430.
- [20] D.R. Olander, W. Siekhaus, R. Jones, J.A. Schwarz, *J. Chem. Phys.* 57 (1972) 408.
- [21] R.T. Yang, C. Wong, *Science* 214 (1981) 437.
- [22] R.T. Yang, C. Wong, *J. Chem. Phys.* 75 (1981) 4471.
- [23] S.M. Lee, Y.H. Lee, Y.G. Hwang, J.R. Hahn, H. Kang, *Phys. Rev. Lett.* 82 (1999) 217.
- [24] A.G. Rinzler et al., *Appl. Phys. A* 67 (1998) 29.
- [25] R.C. Haddon, J. Sippel, A.G. Rinzler, F. Papadimitrakopoulos, *MRS Bull.* 29 (2004) 252.
- [26] R. Khare, S.L. Mielke, J.T. Paci, S. Zhang, R. Ballarini, G.C. Schatz, T. Belytschko, *Phys. Rev. B* 75 (2007) 075412.
- [27] D.W. Brenner, O.A. Shenderova, J.A. Harrison, S.J. Stuart, B. Ni, S.B. Sinnott, *J. Phys.: Condens. Mat.* 14 (2002) 783.
- [28] O.A. Shenderova, D.W. Brenner, A. Omeltchenko, X. Su, L.H. Yang, *Phys. Rev. B* 61 (2000) 3877.
- [29] J.P. Watt, G.F. Davies, R.J. O'Connor, *Rev. Geophys.* 14 (1976) 541.
- [30] N.M. Pugno, *Appl. Phys. Lett.* 90 (2007) 043106.
- [31] M.F. Thorpe, P.N. Sen, *J. Acoust. Soc. Am.* 77 (1985) 1674.
- [32] R. Hill, *J. Mech. Phys. Solids* 13 (1965) 213.
- [33] J.D. Eshelby, *Proc. Roy. Soc. Lond. A* 241 (1957) 376.
- [34] W. Xia, M.F. Thorpe, *Phys. Rev. A* 38 (1988) 2650.
- [35] A.R. Day, K.A. Snyder, E.J. Garboczi, M.F. Thorpe, *J. Mech. Phys. Solids* 40 (1992) 1031.